

Characterisation of the Physical and Geochemical Properties and Infrared Spectra of Five Soil Cores at the AZRI Site Near Alice Springs, Northern Territory

Will Gates, Les Janik, Paul Pavelic, Peter Dillon and Karen Barry

January 2009

Australia is founding its future on science and innovation. Its national science agency, CSIRO, is a powerhouse of ideas, technologies and skills.

CSIRO initiated the National Research Flagships to address Australia's major research challenges and opportunities. They apply large scale, long term, multidisciplinary science and aim for widespread adoption of solutions. The Flagship Collaboration Fund supports the best and brightest researchers to address these complex challenges through partnerships between CSIRO, universities, research agencies and industry.

The Water for a Healthy Country Flagship aims to achieve a tenfold increase in the economic, social and environmental benefits from water by 2025.

For more information about Water for a Healthy Country Flagship or the National Research Flagship Initiative visit www.csiro.au/org/HealthyCountry.html

Citation: Gates W, Janik L, Pavelic P, Dillon P and Barry K. 2009. Characterisation of the Physical and Geochemical Properties and Infrared Spectra of Five Soil Cores at the AZRI Site Near Alice Springs, Northern Territory. CSIRO: Water for a Healthy Country National Research Flagship. 32 pp

Copyright and Disclaimer:

© 2009 CSIRO To the extent permitted by law, all rights are reserved and no part of this publication covered by copyright may be reproduced or copied in any form or by any means except with the written permission of CSIRO.

Important Disclaimer:

CSIRO advises that the information contained in this publication comprises general statements based on scientific research. The reader is advised and needs to be aware that such information may be incomplete or unable to be used in any specific situation. No reliance or actions must therefore be made on that information without seeking prior expert professional, scientific and technical advice. To the extent permitted by law, CSIRO (including its employees and consultants) excludes all liability to any person for any consequences, including but not limited to all losses, damages, costs, expenses and any other compensation, arising directly or indirectly from using this publication (in part or in whole) and any information or material contained in it.

Cover graphic: Mid-Infrared spectra for core samples from depths of 0-10m, at the AZRI site near Alice Springs. *Source: Les Janik, CSIRO Land and Water.*

ACKNOWLEDGEMENTS

The work described here was financially supported by the Power Water Corporation. Core drilling and sample collection was undertaken by Anthony Knapton from the Northern Territory Department of Natural Resources, Environment and the Arts (DNREA).

EXECUTIVE SUMMARY

A sound understanding of the subsurface properties is fundamental in the design and operation of a proposed soil aquifer treatment (SAT) scheme for Alice Springs. SAT can induce biogeochemical processes in the unsaturated and/or saturated zones that can lead to either improvements or deteriorations in water quality, as well as increases or decreases in soil porosity. This report is based upon the physical, geochemical and infrared analyses of up to 92 samples from five cored wells at the AZRI site.

Considerable lateral stratigraphical uniformity was observed between the 5 cores.

The upper 5 m of the soil profile is leached, reducing clay content, capacity to sorb ammonium and salinity. The salt storage in the top 20 m of the soil profile (mainly unsaturated zone) is low to moderate, suggesting the initial increase in groundwater salinity due to infiltration-induced flushing will be negligible.

The clay - and iron oxyhydroxide - rich deeper profile will be advantageous for water quality improvements, particularly for strongly sorbed contaminants such as ammonium and metals. The depth of sorbing layers for ammonium suggest that drying times may need to be extended to allow nitrification between wetting events.

The presence of clayey deposits within the unsaturated zone (peak clay contents range from 20 - 35%) could lead to perching and lateral movement of recharge water that would be problematic if expressed as waterlogging. Related work by Knapton et al, (2006) confirmed that localized perched watertables do developed beneath pilot scale infiltration basins, but rapidly stabilized and did not mound to a degree considered problematic at the test site (adjacent to RN 17940).

Positions for instrumentation in a field trial would need to consider the highly variable drainage characteristics in the profile. In particular, the gravelly layer found at around 7-10 m overlies a more clayey horizon, and has been shown to be a conduit for lateral spreading (Knapton et al, (2006).

Infrared spectra are strongly correlated to soil property data; most notably for variables such as texture, cation exchange capacity, exchangeable cations and clay mineralogy. This suggests that mid infrared analysis could substitute for the more expensive analyses, at least for samples within this calibration soil set. Further calibration with larger sample sets would be required to substitute infrared analysis for conventional measurements for a wider range of soils.

CONTENTS

Acknowledgements	iii
Executive Summary.....	iv
1. Introduction	1
2. Soil Core Collection	1
3. Soil Core Processing	3
4. Analysis.....	3
5. Results	4
6. Conclusions	13
Appendices	15
References	26

LIST OF FIGURES

Figure 1. Study site within the Arid Zone Research Institute showing location of five cored wells	2
Figure 2. Textural analysis of core 17939.....	6
Figure 3. Physical and chemical data for core 17939.....	7
Figure 4. MIR spectra for depths of 0-10m, 10-20m and 20-25m for all core samples.	8
Figure 5. MIR PCA of the spectral data for the 43 samples scanned by FTIR showing (a) the first three PCA loadings: loading-1 (blue), loading-2 (red) and loading-3 (green), and (b) the grouping of the sample spectra according to the score-2 versus score-1 map for cores 17936, 17937, 17938, 17939 and 17940	10
Figure 6 MIR spectra of samples distributed within the four quadrants of the PCA score 1 versus score 2 map.....	11

LIST OF TABLES

Table 1. Summary of cored wells (from Knapton and Lennartz, 2004)	3
Table 2 Results of the PLS cross-validation regression analysis for soil properties, with statistics for N (the number of samples), F (the number of PLS factors or terms used), R^2 (the coefficient of determination), SECV (the standard error of cross-validation), and the regression slope, offset, bias and RPD (residual predictive deviation).....	12

1. INTRODUCTION

Soil Aquifer Treatment (SAT) can lead to either improvements or deteriorations in water quality as recharge water infiltrates through the unsaturated zone and migrates towards points of recovery in the saturated zone (Knapton *et al*, 2004). Water quality changes often involve complex abiotic or biotic processes that occur through interactions between the injected water and soil/aquifer minerals. Deteriorations can arise from the leaching of minerals such as iron/manganese or salts through dissolution or weathering, precipitation of carbonates, phosphates or iron/manganese oxides or dispersal of clays (Bouwer, 1996; Banin *et al*, 2002). Improvements occur through a reduction in the concentrations of contaminants in infiltrating water through physical, chemical and microbiological processes. Thus, particulates can be filtered out, transport of inorganic and organic pollutants can be retarded through adsorption on the soil matrix, organic pollutants can be degraded by soil microorganisms and pathogenic bacteria, viruses and protozoa are attenuated by adsorption, predation by indigenous bacteria and die-off (National Research Council, 1994). Many of these processes occur naturally through diffuse recharge but are greatly enhanced by the higher hydraulic loadings induced by SAT and the contrasting chemical characteristics between the recharge water and the ambient soil - or ground- water.

The success of a pilot-scale SAT trial with reclaimed water at Alice Springs in the Northern Territory relies on defining the appropriate level of risk, and implementing measures to mitigate the risk. Issues that drive this study include:

- 1) the potential for changes in soil structure due to sodicity (geochemical clogging),
- 2) the potential for negative impacts on water quality due to (bio)geochemical reactions and the leaching of accumulated salt, and
- 3) the need to identify locations for placement of monitoring equipment; piezometers, tensiometers, soil moisture measurement and soil solution sampling equipment.

The aim of this work is:

- 1) to collect baseline data to characterise the physical and geochemical properties of core samples collected from five wells in an area targeted for SAT investigations near Alice Springs in the Northern Territory (Knapton and Lennartz, 2004), and
- 2) to determine the Infrared (IR) spectra on subsamples of core material and relate appropriate parts of the IR spectra to the measured soil properties, thus identifying the potential for IR to be used as a low-cost predictor of these variables for future sampling.

2. SOIL CORE COLLECTION

Coring was undertaken during the drilling of five monitoring wells in August-September 2003 at localities selected by DNREA as part of their site characterisation investigations (Knapton and Lennartz, 2004). These wells, identified as RN17936 through to RN19740, are located along a 2 km transect at the Arid Zone Research Institute (AZRI) site near of Alice Springs as shown in **Figure 1**. Summary data are given in **Table 1**. Mud rotary core samples (using a 100mm diameter, 3 m long core barrel) were collected from 5.5 - 30 m below ground level (BGL). Sample return of 70% was generally observed until sand and gravel bands were encountered. Through these sections little to no sample was retrieved. Drilling fluid was composed of cuttings and thickened with biodegradable polymer. Air drilled samples were collected in the top 5 m of the profile during the installation of the surface casing. Core

sections and surficial samples were transported by road to Adelaide for analysis and were received in an air-dry state.

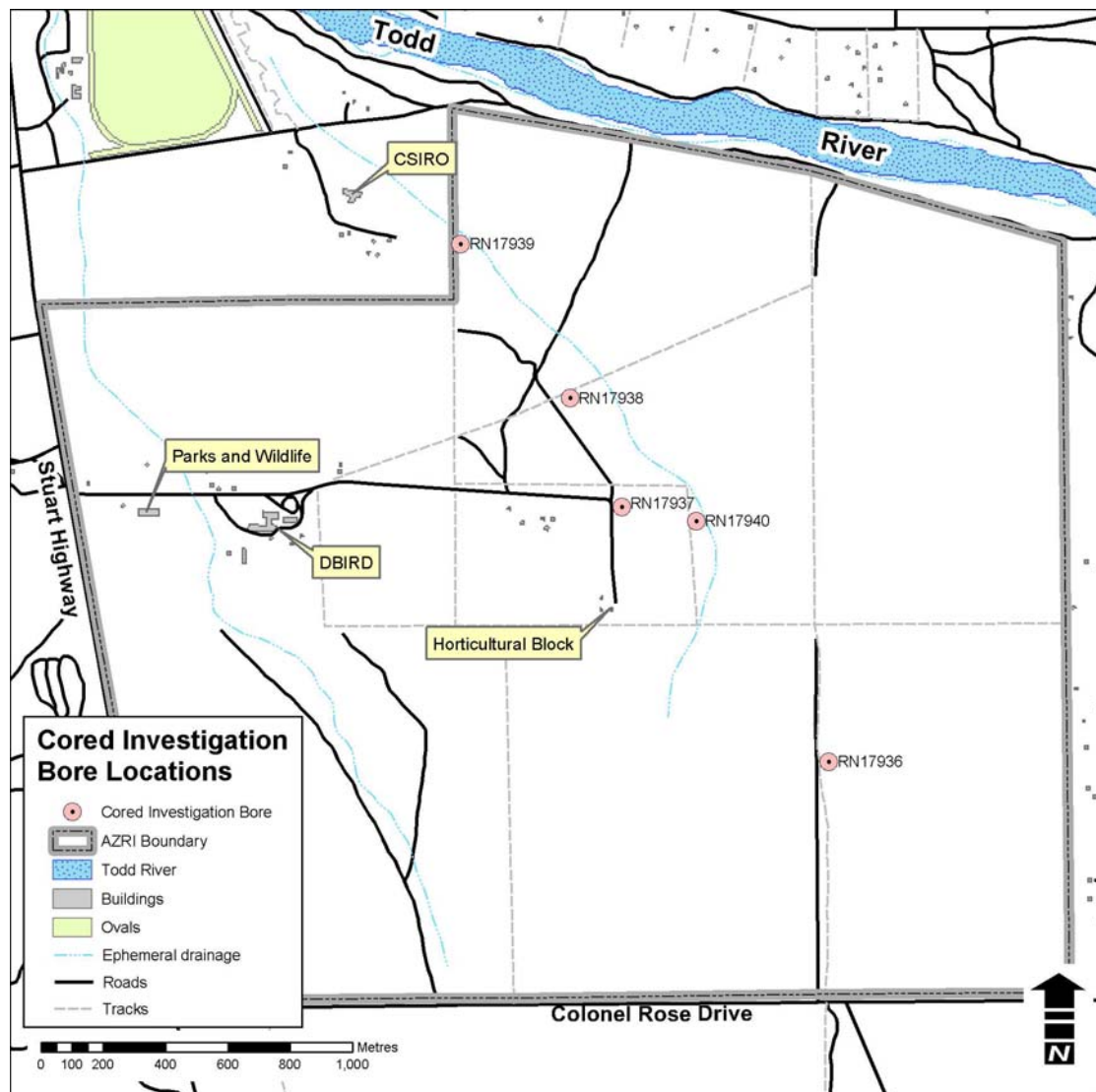


Figure 1. Study site within the Arid Zone Research Institute showing location of five cored wells. The township of Alice Springs is situated around 5 km to the northwest (after Knapton and Lennartz, 2004)

Table 1. Summary of cored wells (from Knapton and Lennartz, 2004)

Well RN ¹	Easting ²	Northing ²	SWL ³ (m BGL)
17936	387655.8	7370333.4	16.1
17937	386990.4	7371152.9	14.42
17938	386824.7	7371501.9	12.6
17939	386473.5	7371996.8	9.07
17940	387229.3	7371107.7	16.11

¹ Wells were drilled to a total depth of 30.1m

² Coordinates are in GDA94 MGA53

³ Depth to groundwater standing water level (SWL) as of 10/2003

3. SOIL CORE PROCESSING

The as-received subsurface core sections were crushed prior to physico-chemical analysis and for Mid-infrared (MIR) and XRD analysis. Most of the surface samples (0-5 m) were dried at 60°C prior to sub-sampling. A total of 92 core sections were variously examined for chemical/physical determinations. A subset of 43 finely ground samples was submitted for MIR analysis, with 22 of these also used for XRD analysis for regression modelling with the MIR spectral data. For chemical and physical analyses (CSIRO Land and Water Analytical Chemistry Unit), each sample was ground and separated to determine the >2 mm content and then oven dried. The <2 mm fraction was used for the appropriate analyses.

4. ANALYSIS

All sections of each core were examined for: electrical conductivity (EC), pH (1:5 soil:water as well as with 0.01 CaCl₂), organic C, CO₃ as free CaCO₃, textural and coarse fragments. Selected core sections were examined for: exchangeable cations (Ca, Mg, Na, K), cation exchange capacity (CEC) performed using NH₄, exchangeable sodium percentage (ESP), sodium absorption ratio (SAR), soluble salts (Ca, Mg, Na, K, S). Most XRD analyses were conducted on core 17939 to serve as a MIR partial least-squares (PLS) calibration training set. Due to drilling fluid disturbance of the samples during coring and air drying afterwards it was considered that hydraulic conductivity measurements could not be related to in-situ conditions so these measurements were not performed.

All samples for MIR analysis were fine-ground for 60 seconds in a steel vibrating puck mill, without sieving, and spectra recorded on a Perkin-Elmer *Spectrum-One* FTIR spectrometer from 450 to 7800 cm⁻¹ (MIR through to the near-infrared NIR) using a diffuse reflectance cell. Spectra were imported into UNSCRAMBLER™ (Camo AS) format for chemometric PLS analysis using the “leave-one-out” cross-validation method (Esbensen, 2002). The optimum number of factors for each component was automatically suggested by the UNSCRAMBLER™ algorithm, and was close to that producing close to the minimum cross-validation error.

For XRD, samples were pre-ground for 15 seconds in a tungsten carbide mechanical mill to pass through a 0.5mm sieve. Two 1g sub-samples were further ground for 10 minutes in a McCrone micronizing mill under ethanol. The resulting slurries were oven dried at 60°C then thoroughly mixed in an agate mortar and pestle before being lightly pressed into aluminium sample holders for X-ray diffraction analysis.

5. RESULTS

Geological and geophysical logs for the five cored wells are given in Appendix 1. Tabulated geochemical and mineralogical data are given in Appendix 2. Photographs for core 17939 prior to sub-sampling are shown in Appendix 3.

Lithology data

The following brief geological description of the AZRI site is taken from the work of Knapton and Lennartz, (2004). The stratigraphy is characterised by a Quaternary palaeochannel feature incised into Tertiary clays and overlain by finer textured deposits. Relatively impervious basal clay occurs from between 18 m BGL where the palaeochannel is absent and 36 m BGL where the channel is present.

The Tertiary clay is described as pale and multi-coloured clays with minor sandy horizons. The palaeochannel feature consists of inter-layered gravels, fine to coarse grained sands and clay sediments 18-36 m BGL. A relatively consistent sequence of fine-grained sediments (silt and fine grained sand) occur from 12-18 m BGL. Inter-layered medium to very coarse grained sediments occur from 0-12 m BGL. The upper portion of the profile (0-3 m BGL) is highly variable.

Textural analyses on <2 mm fractions gave average compositions (with depth and across cores) of coarse gravelly sandy loam: 70% sand, 9% silt and 21% clay, although considerable variability existed (e.g. range in clay was 1-58%). Textural analysis with depth for core 17939 (Figure 2) was very typical (71% sand, 9% silt, 20% clay). With the exception of the 20.9-21 m section, clay contents were $\geq 20\%$ between 4 to 24.6 m for core 17939, with as much as 45% clay at 18-18.1 m depth. Substantial smectitic clays occurred between 2 to 22 m in cores 17937, 17938 and 17939. Coarse fragments (>2 mm) ranged from <1% (non gravelly) to as high as 73% (very gravelly).

The five stratigraphic profiles, all collected from within the palaeochannel, are surprisingly well correlated given the high degree of variability exhibited within any individual profile. These profiles are also relatively consistent with the descriptions of the nearby Inner Farm Basin as presented by Berry (1991).

Geochemical and mineralogical data

Qualitatively XRD analyses indicate significant carbonates at depth (~20 m, 4-11 m below the October 2003 water table). In all core sections studied, Ca^{2+} dominated the exchange complex: for core 17939, Ca^{2+} occupied ~ 50-80% of the complex (Figure 3a). In contrast, Na^+ dominated the soluble salt cation fraction (Figure 3b). Interestingly, exchangeable Ca^{2+} tended to be highest when soluble Na^+ and S were high. Sulfur tended to follow Na^+ trends throughout the profile of core 17939 (Figure 3b).

Generally the CEC measured by NH_4^+ exchange was equal to the sum of the exchangeable cations measured. The exceptions were the near-surface sections (0-6 m) indicating that some weathering has occurred in the upper profile (Figure 3a). It is possible that exchangeable Al^{3+} , oxyhydroxides of iron or kaolin minerals are contributing to this difference, although the pH values (see below) indicate that weathering is not severe.

CEC values ranged from very low to moderately high, indicating a range in mineralogy consistent with the particle size estimations: CEC values were generally highest for those samples with less than ~55% sand. A CEC bulge is evident in core 17939 (Figure 3a) and is indicative of a weathered upper profile.

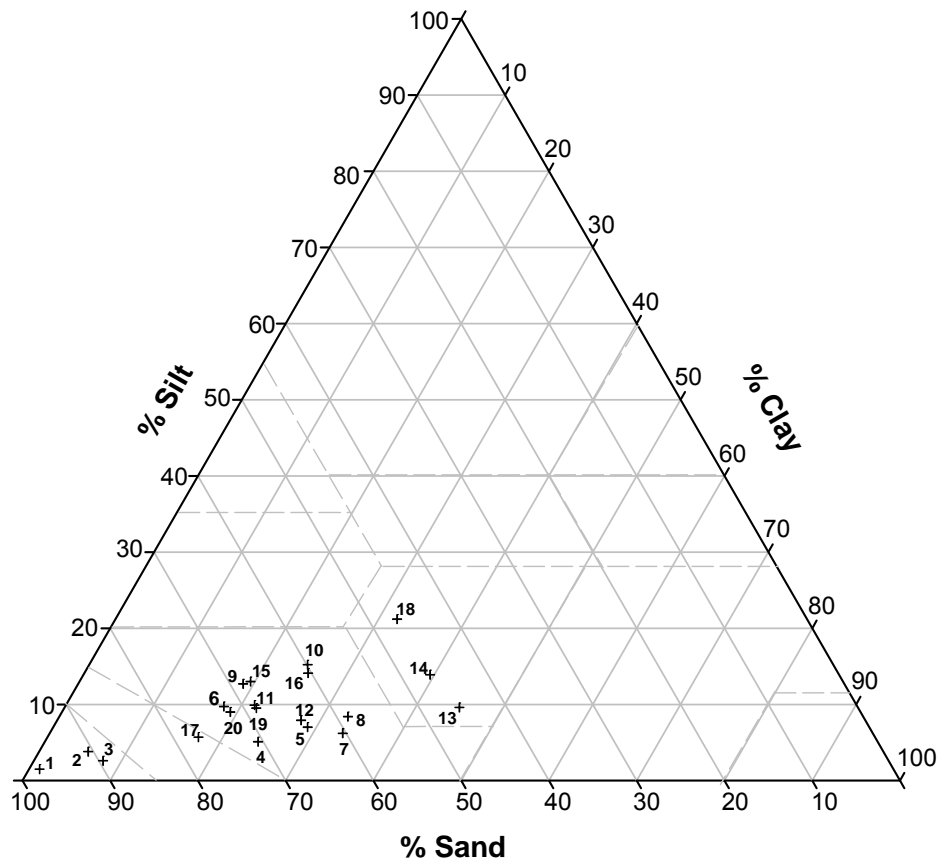
As expected, the sodium absorption ratio (SAR, 1:5 soil:water) (Figure 3c) and exchangeable sodium percentage (ESP) (Figure 3e) were generally elevated with soluble Na^+ : all measures showed two concentration bulges between 5-6 m and 14.7-14.8 m and 14.7-14.8 m and 20-20.15 m depth in core 17939. The electrical conductivity (1:5 soil:water) values (Figure 3d) for core 17939 indicate slight to moderate salinity. However, ESP values are high (>6 %) throughout the upper 24 m of core 17939 (Figure 3e). Thus, in sections where clay content exceeds ~20% inherent sodicity may impact drainage characteristics.

Soil reaction (pH) was reasonably invariable with depth, but in general pH values between 8.0 and 8.5 are consistent with a matrix dominated by calcium carbonate, pH values near neutral consistent with gypsum and pH values >8.5 with bicarbonate (Figure 3c). In core 17939, some sections yielded 1:5 soil:water reactions consistent with a matrix dominated by bicarbonate, but these values followed an opposing trend to soluble Na^+ (i.e., when soluble Na^+ was high, the 1:5 pH was closer to neutral). Available data indicates that S is relatively high when near neutral pH. This may suggest that gypsum could play an important role in buffering pH and alleviating the effects of sodicity in certain sections. Carbonate (as free CaCO_3) was low (generally < 1-2%), but was substantial (as high as 30%) in lower sections of core 17939 (Figure 3e).

Oxalate and dithionite extractable Al^{3+} (Figure 3f) were relatively constant throughout (80-570 and 130-670 ppm, respectively in all sections studied). Very low levels (<100 ppm) of oxalate extractable Mn^{2+} were observed to be generally consistent with high levels (>100ppm) of soluble S. In core 17939, oxalate and dithionite extractable Mn^{2+} were 2 to 4 times higher at 15.5-15.6 m, but the available data do not indicate an association with any other chemical signature. Dithionite extractable Fe^{3+} was high, ranging from 8-12% for much of core 17939, indicating a high level of iron oxyhydroxides in these sediments, which is consistent with deep weathering.

The salt storage in the top 20 m of the soil profile is low to moderate, ranging from 50,000 to 200,000 kg TDS /ha for the five cores (calculated assuming TDS = twice the sum of major cations in mg/kg and using bulk density of 1.5 g/cm^3 ; refer to raw data given in Appendix 2).

Core 17939



1 = 1-2m	11 = 16-16.1m
2 = 2-3m	12 = 17-17.1m
3 = 3-4m	13 = 18-18.1m
4 = 4-5m	14 = 19-19.1m
5 = 5-6m	15 = 19.6-19.7m
6 = 10.5-10.6m	16 = 20-20.15m
7 = 11.9-12m	17 = 20.9-21m
8 = 13.3-13.4m	18 = 22-22.1m
9 = 14.7-14.8m	19 = 24.5-24.6m
10 = 15.5-15.6m	20 = 24.9-25m

Figure 2. Textural analysis of core 17939

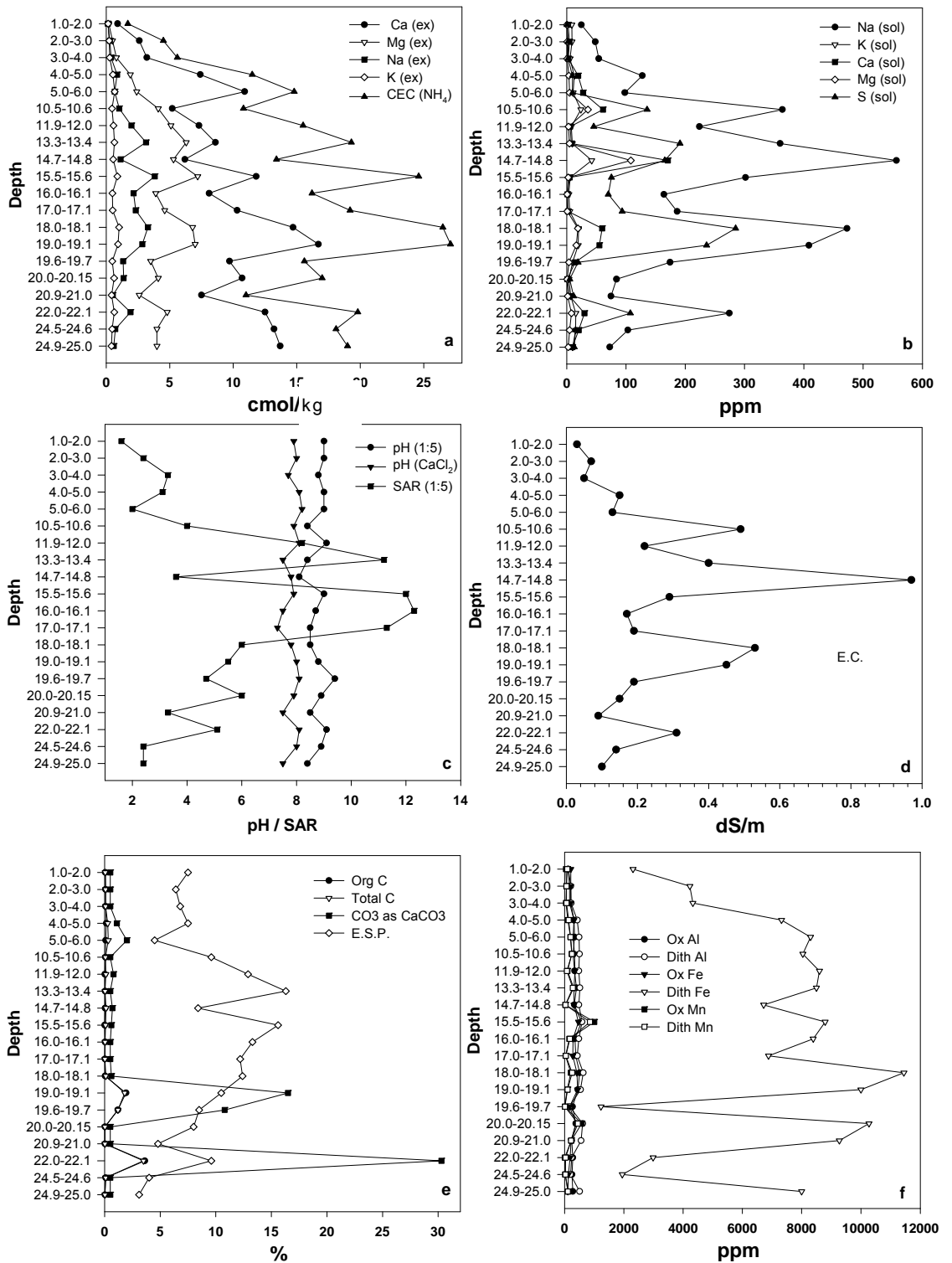


Figure 3. Physical and chemical data for core 17939: a) exchangeable cations and CEC; b) soluble cations and S; c) pH and SAR; d) EC; e) CO₃, organic and total C and ESP; f) oxalate and dithionite extractable Al, Fe and Mn.

Infrared spectral data

Infrared spectra showed significant variation in the major minerals with depth, as illustrated in Figure 4. For example, quartz, smectite and kaolinite, were variable throughout whilst carbonate was high at a depth of about 20 m (see Appendix 2).

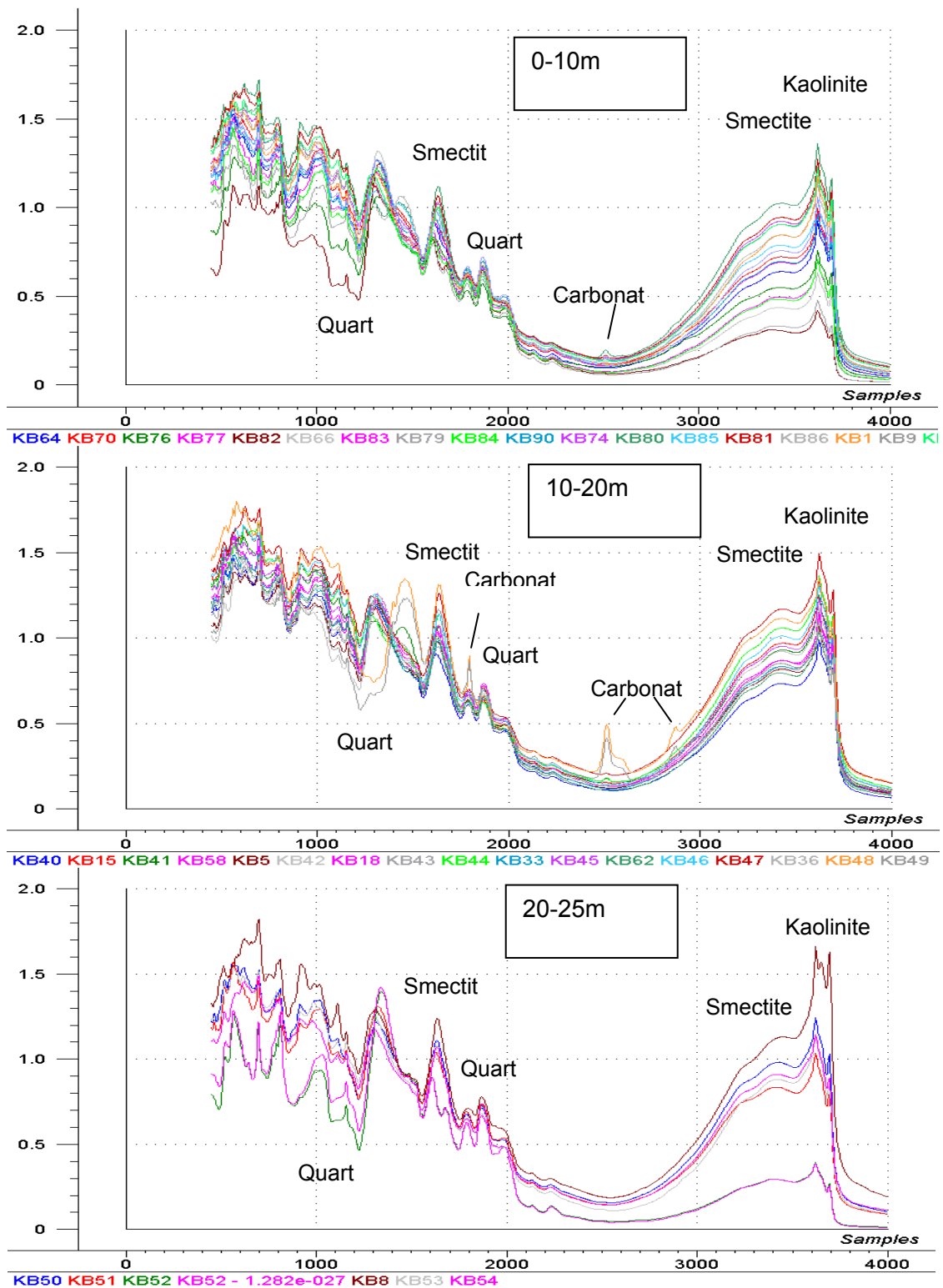
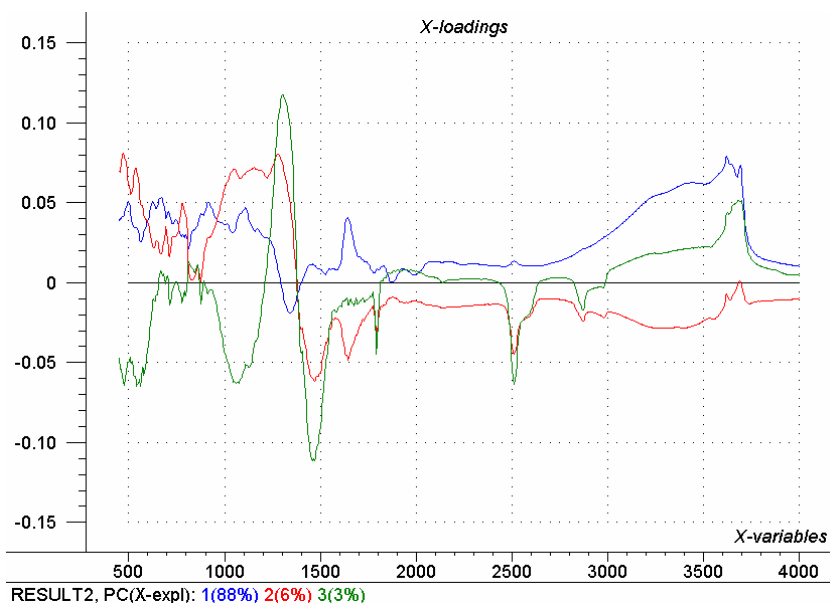


Figure 4. MIR spectra for depths of 0-10m, 10-20m and 20-25m for all core samples. Numerous peaks in the spectral region 450-2000 cm^{-1} were mostly due to quartz, apart from a smectite peak at 1630 cm^{-1} and carbonate near 1810 cm^{-1} .

Carbonate also presented peaks near 2500 and 2900 cm^{-1} , while peaks due to smectite interlayer water could be observed near 3200 and 3400 cm^{-1} . Peaks due to smectite and kaolinite lattice Al-OH vibrations were observed near 3620 and at 2620 - 3695 cm^{-1} respectively. While illite, mica, albite and orthoclase showed large variation with depth according to Appendix 2, these could not be unambiguously identified in the soil spectra.

While visual comparison of the IR spectra showed broad changes due to compositional variation, more subtle relationships and comparisons between the various IR spectra required the use of a more formal mathematical approach. Principal components analysis (PCA) analysis is one such method and can be used to compare spectra according to orthogonal derivations of sub-spectra, known as PCA loadings, common to the entire sample set and related to each soil spectrum by corresponding scaling factors called loading scores. The PCA method and the process of deriving the PCA loadings and scores for the Unscrambler software have been described by many workers including Wold *et al*, (1987) and Esbensen (2002). Peaks in the intensities of the PCA loadings represent the “pure” components or minerals contributing to the soil spectra, with the first PCA loading being the most important and subsequent loadings having decreasing significance. Two-dimensional score versus score plots can thus aid in a formal visual “map” of the relationship or “closeness” between the soil spectra (Janik and Skjemstad, 1995).

For this set of spectral data, the first three PCA spectral loadings suggest that the most important features in the spectra (loading-1) are primarily due to a mixed smectite and kaolinite mineral with very little quartz (see Figure 5a). The second most important feature (loading-2) is due largely to kaolin (possibly halloysite or very poorly ordered kaolinite) and carbonate (negative), while the third loading (loading-3) is mostly due to carbonate (also negative). In general, a positive loading intensity suggests a positive contribution with respect to the mean of the spectra while a negative loading peak suggests an inverse relationship.



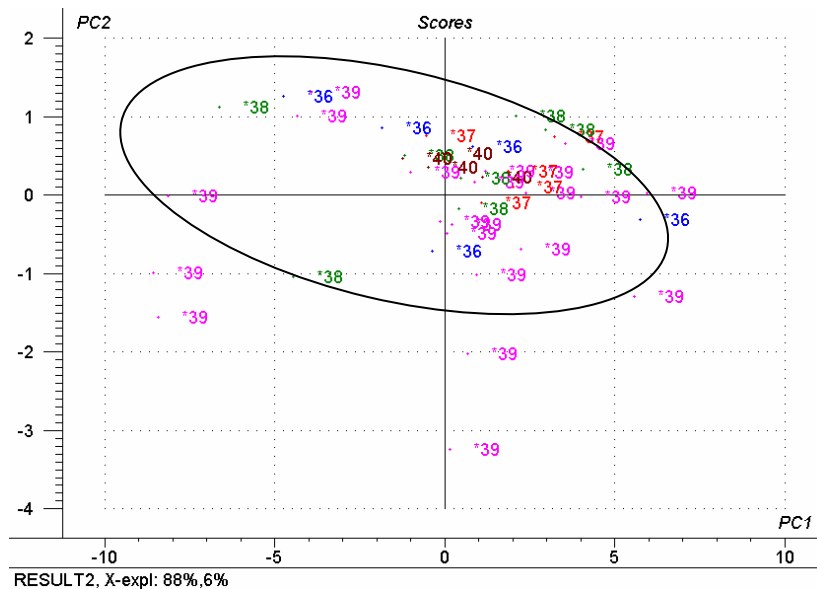


Figure 5. MIR PCA of the spectral data for the 43 samples scanned by FTIR showing (a) the first three PCA loadings: loading-1 (blue), loading-2 (red) and loading-3 (green), and (b) the grouping of the sample spectra according to the score-2 versus score-1 map for cores 17936, 17937, 17938, 17939 and 17940.

The four quadrants of the PCA score map in Figure 5b are characterised by the following assignments:

1. Top Left Quartz, low smectite clay, no carbonate
2. Top Right High clay (smectite/kaolin), low quartz, low carbonate
3. Bottom Left High quartz, low smectite
4. Bottom Right Low quartz, high kaolin/smectite, moderate carbonate.

While most of the samples represented by the score-2 versus score-1 spectral data for the 43 samples scanned by FTIR could be grouped within the ellipse shown in Figure 5b, samples from core 17939 indicated a large variation from the main body within the ellipse. In particular, the significant displacement of about six of the samples from the main body towards large negative score-1 and score-2 values showed these samples to be outliers, representing low concentrations of smectite and high concentrations of carbonate.

The complete set of soil spectra for all the cores are depicted in Figure 6 corresponding to the scores within the quadrants of Figure 5b.

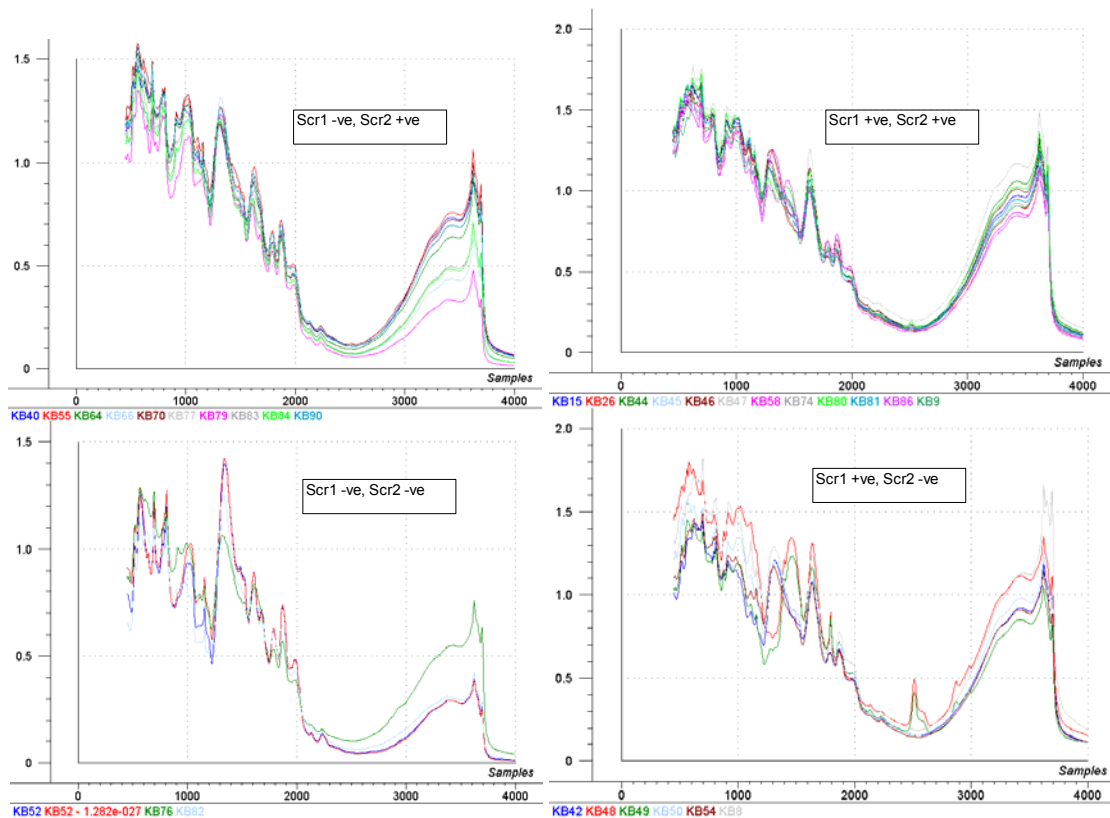


Figure 6 MIR spectra of samples distributed within the four quadrants of the PCA score 1 versus score 2 map

Infrared partial least-squares (PLS) analysis

Infrared partial least-squares (PLS) analysis is a multivariate method commonly used to predict sample properties from multivariate data, including infrared spectra. In this application, PLS models the regression of reference laboratory data against the spectral intensities (along the frequency or wavenumber axis) (Geladi and Kowalski, 1986; Haaland and Thomas, 1987). For soils, the resulting PLS model of regression coefficients and PLS loadings (similar to the PCA loadings but now weighted with respect to the analyte concentrations) for each of the analytes can, in principle, be used for subsequent prediction of similar soil properties from MIR spectra of unknown samples (Janik and Skjemstad, 1995). A separate set of loadings and scores is derived for each analyte of the soil set. As a predictive tool, PLS is superior to univariate methods in that relatively large portions of the spectra can be used for each model (whole spectrum method) rather than just a few peak intensities. Complications can arise, however, due to the degrading influence of spectral data from frequencies that have no correlation with the analyte in question, leading to modelling 'noise'.

For PLS calibration training purposes, in ideal situations where the data set comprises a relatively large number of samples, the full data set can be split into a calibration set (25%), an internal validation set (50%) and an external test set (25%). This results in the least optimistic training statistics and therefore maximum confidence in the PLS model for predictive purposes. Alternatively, the calibration and validation samples can be combined into a "leave-one-out" cross-validation set where each sample is tested by predicting its values from a model of the remaining samples, and then predicting the test set samples. In this present situation, however, there are insufficient samples to create a separate test set and so only a cross-validation could be performed.

For large data sets, relatively large spectral regions can be used for the PLS analysis, allowing a relatively large variation in the data to be modelled, and thereby resulting in a robust calibration. In this analysis however, there are relatively few samples, and individual samples can heavily influence and distort the regression. As an aid to improving the relevance of the spectral information used in the PLS modelling, and thus the accuracy of predictions, those parts of the spectra which bear little if any correlation with the analyte values can be omitted from the calibration. There is therefore an advantage in reducing the “whole spectrum” to a far fewer, and better chosen infrared frequencies, which avoid unusual spectral features unique to these outlier samples. The PLS method used here to optimise the frequencies utilises a “jack-knifing” procedure in the Unscrambler software which tests the influence of each spectral data point on the regression.

Table 2 Results of the PLS cross-validation regression analysis for soil properties, with statistics for N (the number of samples), F (the number of PLS factors or terms used), R² (the coefficient of determination), SECV (the standard error of cross-validation), and the regression slope, offset, bias and RPD (residual predictive deviation).

	N	F	R ²	SECV	Slope	Offset	Bias	RPD
Mn-ox	43	8	0.62	119	0.59	64	-5.90	1.5
Fe-ox	43	8	0.74	52	0.77	64	-3.30	2.0
Al-ox	43	7	0.90	31	0.90	34	1.96	3.2
Sand	43	8	0.90	5.50	0.95	3.50	0.07	2.9
Silt	12	4	0.80	2.35	0.78	2.35	-0.15	2.1
CO ₃	12	4	0.94	2.82	0.90	0.76	0.02	4.1
S sol	43	8	0.88	23	0.84	5.90	-0.81	3.0
Na sol	43	9	0.10	125	0.62	60	8.30	1.1
Mg sol	43	9	0.03	16.00	0.29	4.10	-1.10	1.1
K sol	43	8	0.90	3.90	0.62	4.30	-0.34	2.2
Ca sol	42	8	0.75	14.70	0.58	7.10	-1.30	2.0
SAR	42	9	0.89	1.07	0.84	0.65	0.03	2.8
ESP	43	9	0.90	1.28	0.85	1.00	-0.02	3.1
CEC	43	8	0.90	1.96	0.96	0.67	0.17	3.0
Exch Cats	41	4	0.94	1.45	0.96	0.59	0.05	4.2
pH _{ca}	40	9	0.79	0.20	0.77	1.74	-0.01	2.1
Exch K	41	9	0.82	0.09	0.85	0.08	0.00	2.3
Exch Na	41	9	0.81	0.42	0.82	0.16	0.00	2.2
Exch Mg	41	8	0.87	0.74	0.83	0.52	-0.01	2.6
Exch Ca	41	8	0.91	1.15	0.94	0.54	0.06	3.3
Leco	41	6	0.80	0.15	0.75	0.03	-0.02	5.3
TOC	41	8	0.77	0.17	0.66	0.03	-0.02	4.8
Clay	41	8	0.89	3.76	0.96	0.67	-0.11	2.9
pH _w	41	5	0.31	0.35	0.42	5.05	0.03	1.2
EC	41	2	0.05	0.18	0.10	0.15	0.00	1.0
ADM	39	9	0.84	0.49	0.88	0.29	0.01	2.5
XRD-Quartz	20	7	0.96	2.02	0.96	1.82	0.18	4.9
XRD-Albite	20	8	0.89	0.84	0.83	1.39	0.00	3.0
XRD-Othoclase	20	7	0.94	0.37	0.90	0.44	-0.01	4.0
XRD-Kaolinite	20	9	0.97	0.63	0.96	0.52	0.02	5.5
XRD-illite	20	6	0.95	1.10	0.96	0.35	-0.03	4.6
XRD-Calcite	20	2	0.87	3.49	0.80	0.40	-0.44	2.7
XRD-Calcite(7-F)	20	7	0.96	1.93	0.97	0.12	0.00	4.9
XRD-Smectite	19	7	0.90	2.16	0.84	2.64	0.22	3.3

Table 2 presents the results of the PLS analysis for all the available soil properties for which reference data was provided. In order to reduce the likelihood of overfitting the regressions

(and thus leading to an overly optimistic assessment of the predictive performance of the PLS models), the number of PLS factors required to achieve a minimum prediction error (standard error of cross-validation SECV) was kept to a minimum. In general, the number of PLS factors (F) should be significantly smaller than the number of samples. For this study, with 40-43 samples a maximum of about 10 factors should be used. In fact, for many analytes only about 8-9 factors were required to achieve a minimum calibration error, so that a maximum of 8-9 factors was also used to describe the cross-validation models even though a larger number of factors usually led to a far lower cross-validation error.

In spite of the restriction in the number of PLS factors used, due to the small sample set size, and particularly due to the relatively small variation in sample sources, **there is still a significant chance that the models may be overfitted and not robust**. This is most likely where the model may be heavily leveraged by a few samples. One important statistic used to describe the potential of PLS regression to predict sample values outside the calibration sample set is the residual predictive deviation (RPD) derived from the ratio between the standard deviation for a particular analyte (Std) and the standard error (SEP or SECV) (Cozzolino *et al*, 2005). Values of RPD >3 are considered to be analytically accurate, values between 2 and 3 are semi-quantitative, and 1 to 2 are indicator only. The cross-validation results presented in Table 2 therefore suggest that the MIR PLS method has sufficient potential to be considered for the development of a more comprehensive calibration for soil core analysis.

6. CONCLUSIONS

The main conclusions for this study, drawn from the physical, geochemical and MIR analyses of up to 92 samples from five cored wells to a depth of 30 m at the AZRI site are:

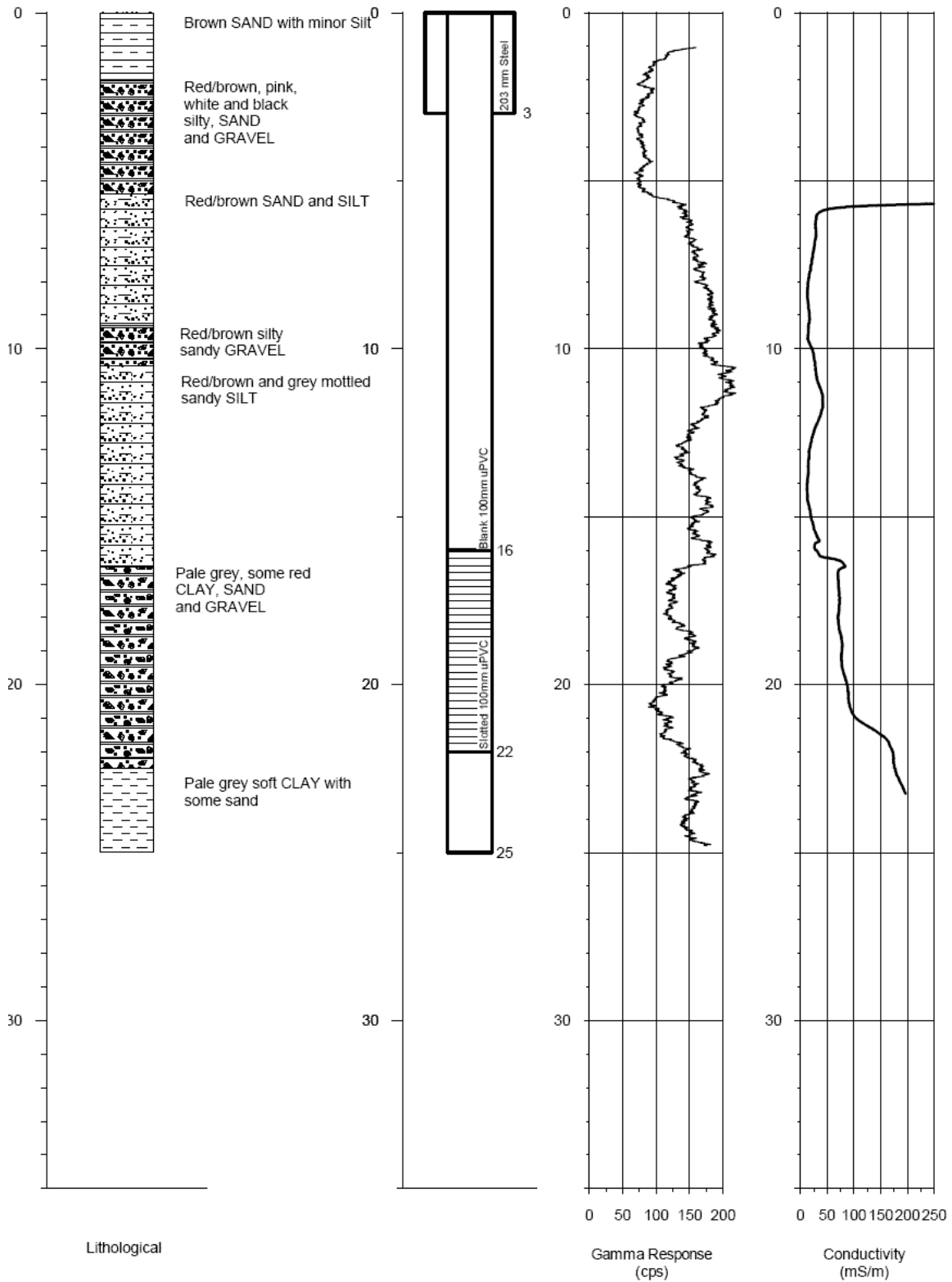
- Clay-rich portions of the profile with high ESP have the potential for sodicity induced clogging, particularly if the recharge water contains a high proportion of monovalent ions.
- The upper 5 m of the soil profile is leached, which had reduced the clay content, salinity and capacity to sorb ammonium.
- The salt storage in the top 20 m of the soil profile (mainly unsaturated zone) is low to moderate, suggesting the initial increase in groundwater salinity due to infiltration-induced flushing will be negligible.
- The clay - and iron oxyhydroxide - rich deeper profile will be advantageous for water quality improvements, particularly for strongly sorbed contaminants such as ammonium and metals. The depth of sorbing layers for ammonium suggest that drying times may need to be extended to allow nitrification between wetting events.
- The presence of clayey deposits within the unsaturated zone (peak clay contents range from 20-35%) could lead to lateral movement of recharge water that would be problematic if mounding was expressed as waterlogging. Related work by Knapton *et al*, (2006) confirmed that localized perched watertables developed beneath pilot scale infiltration basins, but rapidly stabilized and did not mound to a degree considered problematic at the test site (adjacent to RN 17940).
- Positions for instrumentation will need to consider the highly variable drainage characteristics in the profile. In particular, the contrast between the gravelly layer found at around 7-10 m that overlies a more clayey horizon, which has been shown to be a conduit for lateral spreading (Knapton *et al*, 2006).

- Infrared spectra are strongly correlated to soil property data; most notably for variables such as texture, CEC, exchangeable cations and clay mineralogy. This suggests that MIR analysis could substitute for the more expensive analyses, at least for samples within this calibration soil set. Further calibration with larger sample sets would be required to expand this range to other soils sets.

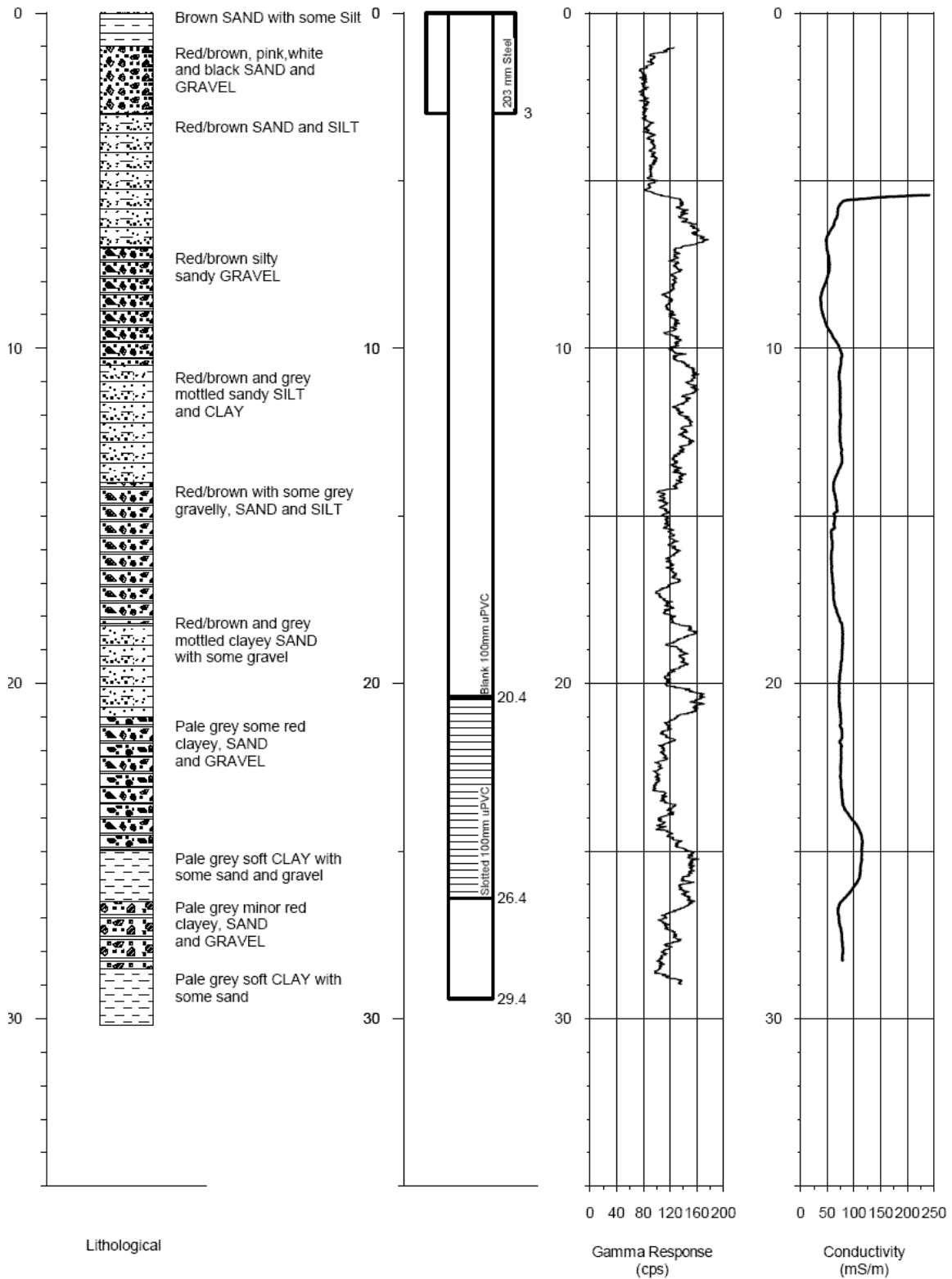
APPENDICES

Geological logs for the five cored wells

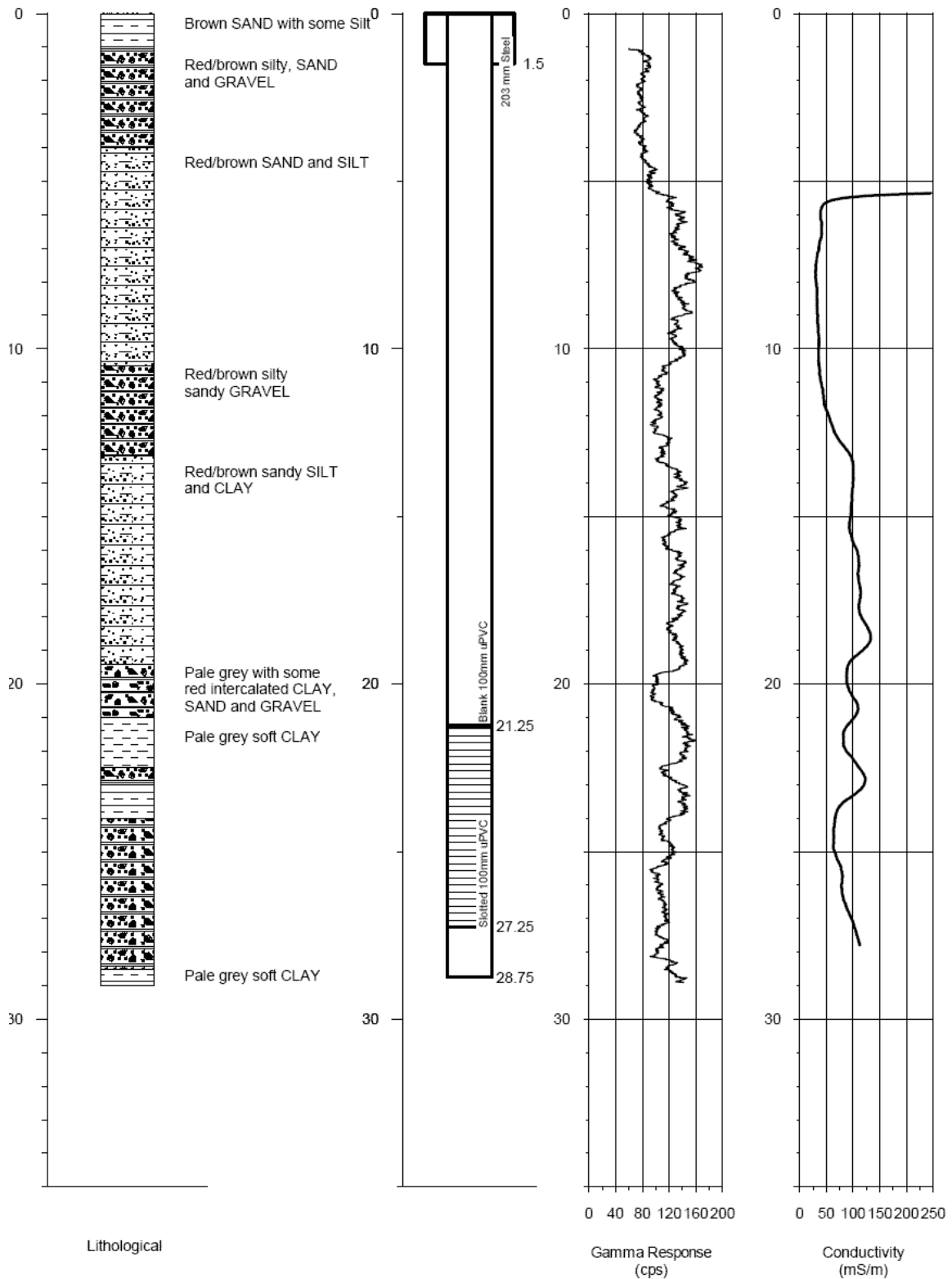
17936

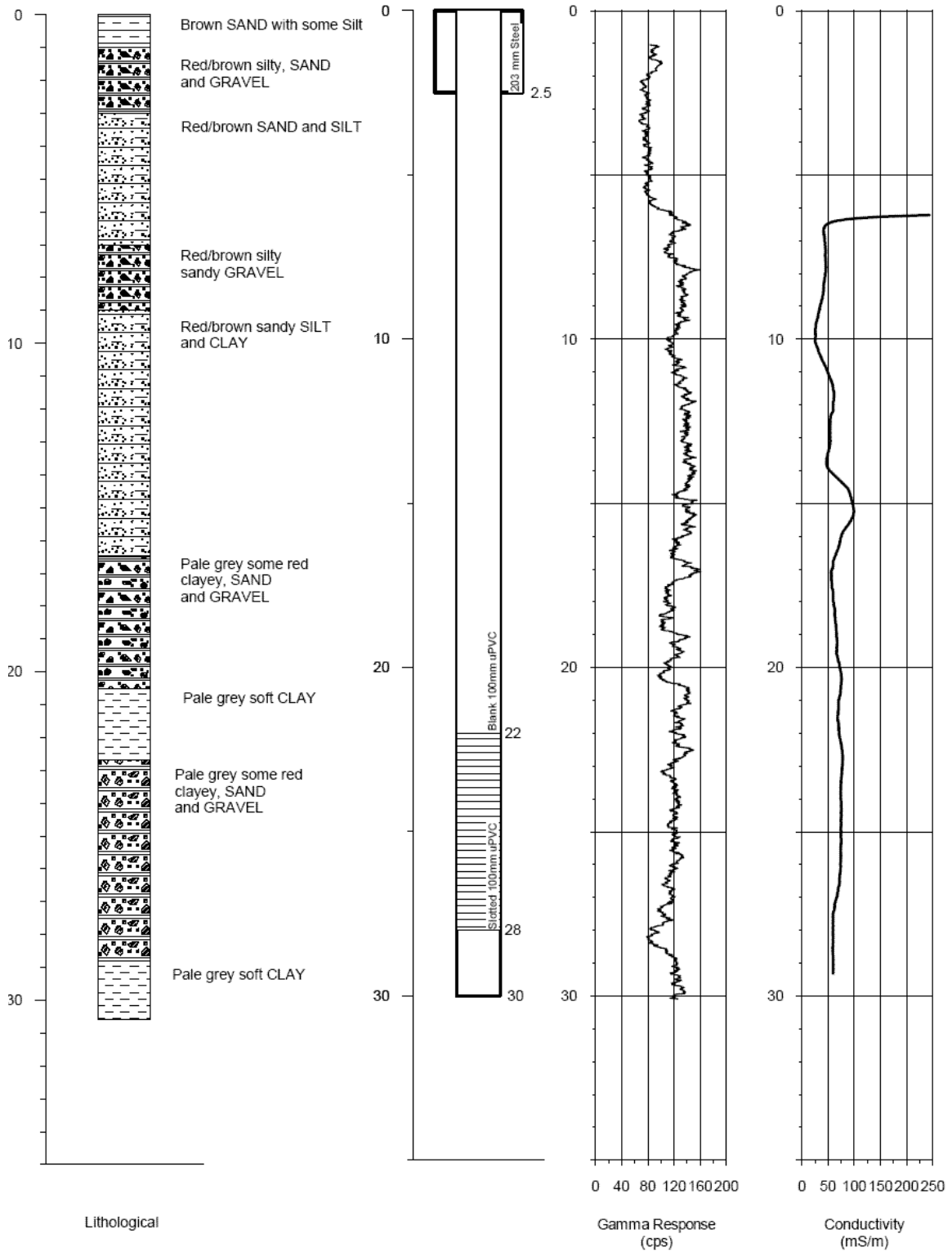


17937

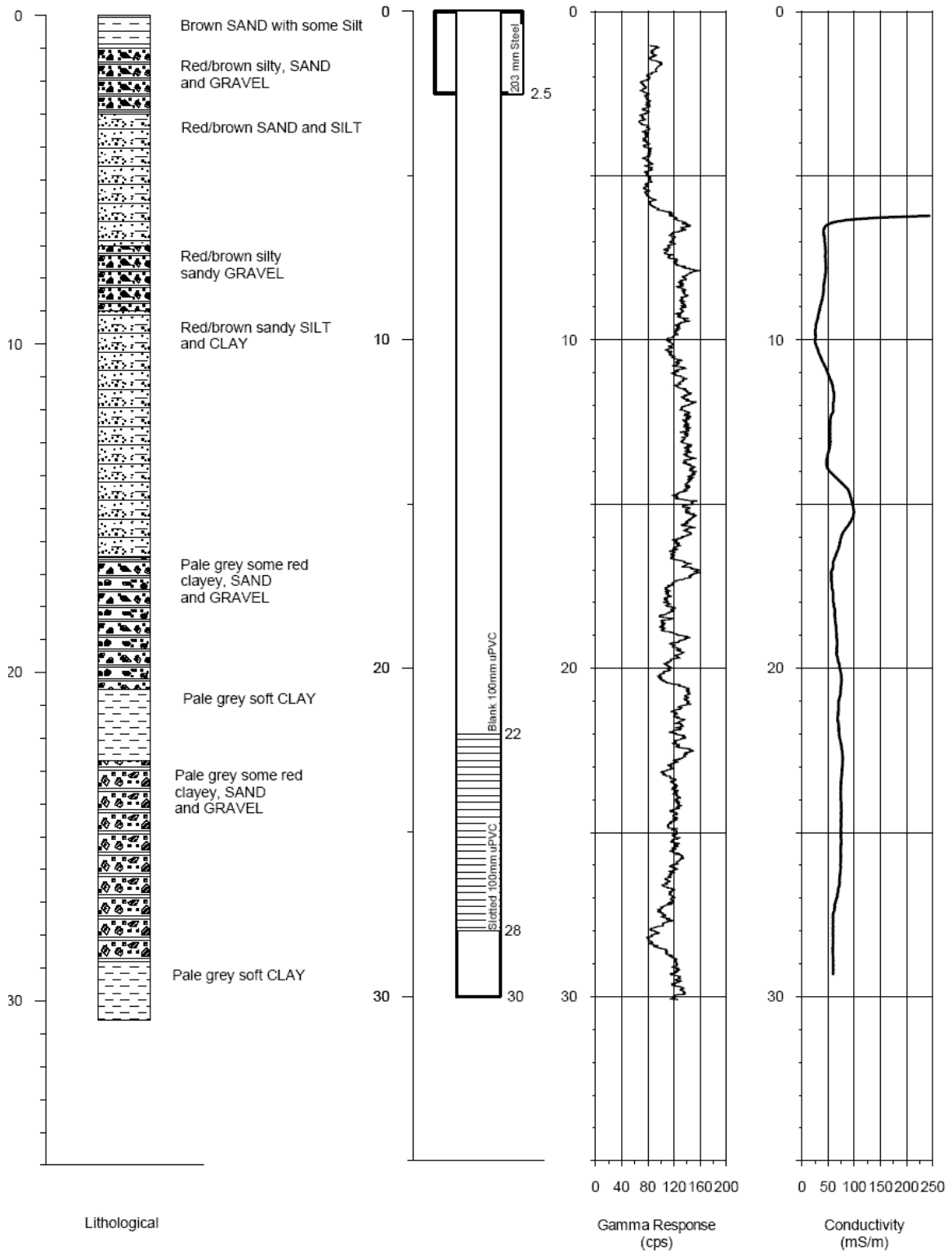


17938





17940



Mineralogical Data

Well RN	Depth (m)	Quartz	Albite	Orthoclase	Kaolin	Illite/Mica	Calcite	Hematite	Smectite	Amphibole
17936	13.0-13.1	51	7	3	14	15	<1	<1	10	-
17937	10.9-11.0	37	10	4	19	17	<1	<1	14	-
17937	18	48	10	8	13	8	<1	<1	11	1
17938	12.9-13.0	45	8	3	14	14	<1	<1	15	<1
17938	15.9-16.0	46	11	6	10	11	<1	<1	15	<1
17938	18.9-19.0	54	10	6	8	11	<1	<1	12	-
17939	10.5-10.6	53	14	5	9	18	<1	<1	-	<1
17939	11.9-12.0	52	8	5	14	14	<1	<1	6	-
17939	13.3-13.4	47	7	4	17	14	<1	<1	10	-
17939	14.7-14.8	44	12	4	16	15	<1	<1	8	<1
17939	15.5-15.6	34	9	3	18	12	<1	<1	23	-
17939	16.0-16.1	48	9	4	14	12	<1	<1	12	<1
17939	17.0-17.1	45	7	5	14	12	<1	<1	17	-
17939	18.0-18.1	42	6	3	14	3	<1	<1	31	-
17939	19.0-19.1	20	3	2	14	3	35	-	23	-
17939	19.6-19.7	42	8	4	7	2	21	-	16	-
17939	20-20.15	58	7	7	11	3	1	<1	14	-
17939	20.9-21.0	58	9	7	8	7	1	-	10	-
17939	22.0-22.1	31	4	3	14	3	19	-	26	-
17939	24.5-24.6	49	10	6	9	7	1	-	18	-
17939	24.9-25.0	45	8	4	11	12	<1	<1	20	-
17940	12.9-13.15	60	8	7	13	7	<1	<1	4	<1

Table A1. Cross reference between infrared sample number, chemical analysis sample number and the well and depth interval




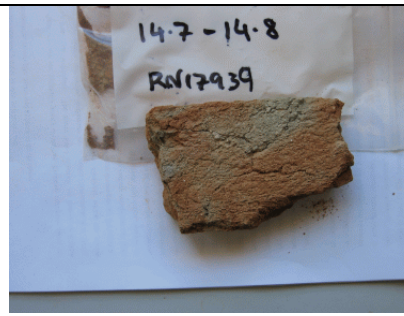


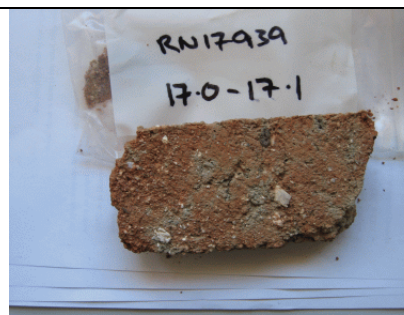
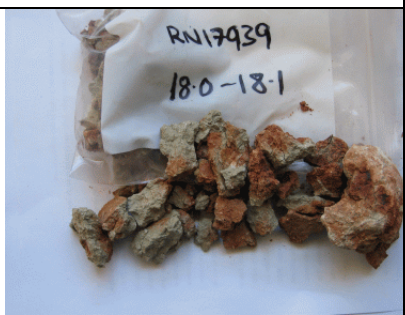
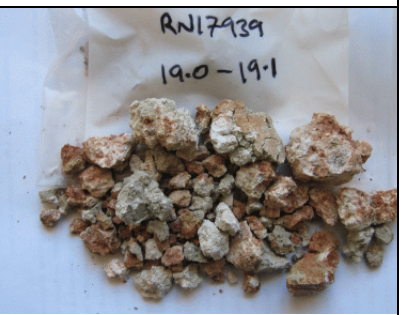
Infrared	ACU No.	Sample ID - well and depth interval (m)
KB1	04ADL 00001	RN17936 5.4-5.5
KB5	04ADL 00005	RN17936 13.0-13.1
KB8	04ADL 00008	RN17936 22.2-22.27
KB9	04ADL 00009	RN17937 5.5-5.6
KB15	04ADL 00015	RN17937 10.9-11
KB18	04ADL 00018	RN17937 14-14.1
KB26	04ADL 00026	RN17938 7.5-7.6
KB33	04ADL 00033	RN17938 15.9-16.0
KB36	04ADL 00036	RN17938 18.9-19.0
KB40	04ADL 00040	RN17939 10.5-10.6
KB41	04ADL 00041	RN17939 11.9-12.0
KB42	04ADL 00042	RN17939 13.3-13.4
KB43	04ADL 00043	RN17939 14.7-14.8
KB44	04ADL 00044	RN17939 15.5-15.6
KB45	04ADL 00045	RN17939 16.0-16.1
KB46	04ADL 00046	RN17939 17.0-17.1
KB47	04ADL 00047	RN17939 18.0-18.1
KB48	04ADL 00048	RN17939 19.0-19.1
KB49	04ADL 00049	RN17939 19.6-19.7
KB50	04ADL 00050	RN17939 20.0-20.15
KB51	04ADL 00051	RN17939 20.9-21.0
KB52	04ADL 00052	RN17939 22.0-22.1
KB53	04ADL 00053	RN17939 24.5-24.6
KB54	04ADL 00054	RN17939 24.9-25.0
KB55	04ADL 00055	RN17940 9.0-9.1
KB58	04ADL 00058	RN17940 12.9-13.15
KB62	04ADL 00062	RN17940 16.4-16.5
KB64	04ADL 00064	RN17936 0-1.0
KB66	04ADL 00066	RN17936 2.0-3.0
KB70	04ADL 00070	RN17937 0-1.0
KB74	04ADL 00074	RN17937 4.0-5.0
KB76	04ADL 00076	RN17938 0-1.0
KB77	04ADL 00077	RN17938 1.0-2.0
KB79	04ADL 00079	RN17938 3.0-4.0
KB80	04ADL 00080	RN17938 4.0-5.0
KB81	04ADL 00081	RN17938 5.0-6.0
KB82	04ADL 00082	RN17939 1.0-2.0
KB83	04ADL 00083	RN17939 2.0-3.0
KB84	04ADL 00084	RN17939 3.0-4.0
KB85	04ADL 00085	RN17939 4.0-5.0
KB86	04ADL 00086	RN17939 5.0-6.0
KB90	04ADL 00090	RN17940 3.0-4.0

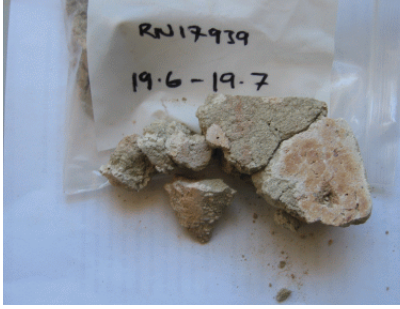


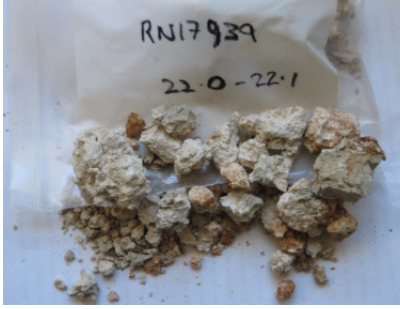


Summary statistics of chemical and mineralogical data

	Min	Max	Mean	SDev
Mn-ox	6	1000	170	183
Fe-ox	80	510	293	103
Al-ox	80	570	322	98
Sand	31	98	67	16
Silt	1.5	23.0	9.9	5.0
CO3	0.56	30.28	8.01	11.52
S sol	0.84	285.02	41.49	68.58
Na sol	0.79	556.19	135.79	131.94
Mg sol	0.59	108.19	7.29	16.99
K sol	3.33	43.5	12	8.45
Ca sol	0.86	170.61	19.85	28.69
SAR	0.82	12.29	3.82	3.01
ESP	0.11	16.25	6.68	4.00
CEC	1.75	27.05	13.95	5.96
Exch Cats	1.33	27.50	13.36	6.15
pHca	6.27	8.26	7.71	0.43
Exch K	0.12	1.12	0.54	0.21
Exch Na	0.01	3.83	0.99	0.94
Exch Mg	0.17	7.18	3.14	1.91
Exch Ca	0.86	16.74	8.69	3.85
Leco	0.02	3.61	0.35	0.80
TOC	0.01	3.61	0.32	0.81
Clay	1.15	57.77	22.15	10.92
pHw	7.26	9.36	8.69	0.41
EC	0.029	0.965	0.173	0.176
ADM	0.26	6.09	2.33	1.21
XRD-Quartz	20	60	46	10
XRD-Albite	3	14	8	3
XRD-Othoclase	2	7	5	2
XRD-Kaolinite	7	19	13	3
XRD-Illite	2	18	10	5
XRD-Calcite	0.51	35	4.26	9.38
XRD-Calcite(7-F)	0.51	35	4.26	9.38
XRD-Smectite	4	31	15	7

Appendix 3

Photographs of core samples from RN 17939

		
10.5-10.6 m	11.9-12.0 m	13.3-13.4 m
		
14.7-14.8 m	15.5-15.6 m	16.0-16.1 m
		
17.0-17.1 m	18.0-18.1 m	19.0-19.1 m

		
<p style="text-align: center;">19.6-19.7 m</p>	<p style="text-align: center;">20.0-20.15 m</p>	<p style="text-align: center;">20.9-21.0 m</p>
		
<p style="text-align: center;">22.0-22.1 m</p>	<p style="text-align: center;">24.5-24.6 m</p>	<p style="text-align: center;">24.9-25.0 m</p>

REFERENCES

- Banin, A., Lin, C., Eshel, K.E., Roehl, I., Negev, I., Greenwald, D., Shachar, Y. and Yablekovitch, Y. (2002) Geochemical processes in recharge basin soils used for municipal effluents reclamation by the soil-aquifer treatment (SAT) system. In: Management of Aquifer Recharge for Sustainability, P.J. Dillon (Ed.) *Proceedings of the 4th International Symposium on Artificial Recharge (ISAR4)*, Adelaide Sept. 22-26, 2002, Swets & Zeitlinger, Lisse, ISBN. 90 5809 527 4, pp.327-332.
- Berry, K. (1991) Monitoring Development Alice Springs Commonage. Power and Water Authority Report 02/1991A.
- Bouwer, H. (1996) Issues in artificial recharge. *Water Science and Technology* 33:381-390.
- Cozzolino, D., Montossi, F. and San Julian, R. (2005). The use of visible (VIS) and near infrared (NIR) reflectance spectroscopy to predict fibre diameter in both clean and greasy wool samples. *Animal Science*, **80**, 333-337.
- Esbensen, K. (2002). "Multivariate Data Analysis - In Practice", ISBN 82-993330-3-2, CAMO Process AS, Oslo, 5th Edition.
- Geladi, P. and Kowalski, B.R. (1986). Partial least-squares regression: a tutorial, *Anal. Chim. Acta.* **185**, 1–17.
- Haaland, D.M. and Thomas, V.T. (1988). Partial Least-squares methods for spectral analyses. 1. Relation to other quantitative calibration methods and the extraction of qualitative information. *Anal. Chem. J.* **60**, 1193-1202.
- Janik, L.J. and Skjemstad, J.O. (1995). Characterization and analysis of soils using mid-infrared partial least squares. II. Correlations with some laboratory data. *Aust. J. Soil Res.* **33**, 637-650.
- Knapton, A., Jolly, P., Pavelic, P., Dillon, P., Barry, K., Mucha, M. and Gates, W. (2004) Feasibility of a pilot 600 ML/yr Soil Aquifer Treatment Plant at the Arid Zone Research Institute. Department of Infrastructure, Planning and Environment, Alice Springs, Report No. 29/2004A.
- Knapton, A., Pavelic, P., Dillon, P. and Low, B. (2006) Field infiltration tests with potable water to predict hydraulic behaviour of a soil aquifer treatment trial for Alice Springs, Northern Territory. Department of Infrastructure, Planning & Environment Conservation and Natural Systems Technical Report No. 28/2005A.
- Knapton, A. and Lennartz, R. (2004) Alice Springs Water Reuse Scheme, Soil Aquifer Treatment Project - Volume 1 Site Characterisation, Department of Infrastructure, Planning and Environment, Alice Springs, Report No WRA 26/2005.
- National Research Council, (1994) Groundwater Recharge Using Waters of Impaired Quality. National Academy Press, Washington DC.
- Wold, S., Esbensen, K. and Geladi, P. (1987). Principal component analysis - A tutorial, *Chemom. Intell. Lab. Syst.*, **2**, 37 - 52.



Contact Us

Phone: 1300 363 400

+61 3 9545 2176

Email: enquiries@csiro.au

Web: www.csiro.au

Your CSIRO

Australia is founding its future on science and innovation. Its national science agency, CSIRO, is a powerhouse of ideas, technologies and skills for building prosperity, growth, health and sustainability. It serves governments, industries, business and communities across the nation.